Toxicon 117 (2016) 1–12

Contents lists available at ScienceDirect

Toxicon

journal homepage: www.elsevier.com/locate/toxicon

Biochemical and functional studies of ColTx-I, a new myotoxic phospholipase A_2 isolated from *Crotalus oreganus lutosus* (Great Basin rattlesnake) snake venom

J.R. Almeida [a, d, e], L.M. Resende [a], A.G. Silva [c], R.I.M.A. Ribeiro [c], R.G. Stábeli [b, e], A.M. Soares [b, e], L.A. Calderon [b, e], S. Marangoni [a], S.L. Da Silva [d, e, *]

[a] Department of Biochemistry and Tissue Biology, Institute of Biology, Campinas State University (UNICAMP), Campinas, SP, Brazil
[b] Oswaldo Cruz Fundation (FIOCRUZ), CEBio, Fiocruz Rondônia and Federal University of Rondônia, Porto Velho, RO, Brazil
[c] CCO, Universidade Federal de São João del Rei, Divinópolis, MG, Brazil
[d] IKIAM – Universidad Regional Amazónica, Tena, Napo, Ecuador
[e] International Network of Ecuadorian Snakes Venoms Studies (RIEVSE), Ecuador

ARTICLE INFO

Article history:
Received 29 October 2015
Received in revised form
5 March 2016
Accepted 15 March 2016
Available online 17 March 2016

Keywords:
Snake venom
Phospholipase A_2
Myotoxin
Crotalus oreganus lutosus
Biological activities

ABSTRACT

Commonly, phospholipases A_2 (PLA_2s) play key roles in the pathogenesis of the local tissue damage characteristic of crotaline and viperine snake envenomations. *Crotalus oreganus lutosus* snake venom has not been extensively studied; therefore, the characterization of its components represents a valuable biotechnological tool for studying pathophysiological processes of envenoming and for gaining a deeper understanding of its biological effects. In this study, for the first time, a basic PLA_2 myotoxin, ColTx-I, was purified from *C. o. lutosus* through two chromatographic steps. ColTx-I is monomeric with calculated molecular mass weight (Mw) of 14,145 Da and a primary structure closely related to basic PLA_2s from viperid venoms. The pure enzyme has a specific activity of 15.87 ± 0.65 nmol/min/mg at optimal conditions (pH 8.0 and 37 °C). ColTx-I activity was found to be dependent on Ca^{2+}, as its substitution by other ionic species as well as the addition of chelating agents significantly reduced its phospholipase activity. *In vivo*, ColTx-I triggered dose-dependent inflammatory responses, measured using the paw edema model, with an increase in IL-6 levels, systemic and local myotoxicity, characterized by elevated plasma creatine kinase activity. ColTx-I induced a complex series of degenerative events associated with edema, inflammatory infiltrate and skeletal muscle necrosis. These biochemical and functional results suggest that ColTx-I, a myotoxic and inflammatory mediator, plays a relevant role in *C. o. lutosus* envenomation. Thus, detailed studies on its mechanism of action, such as evaluating the synergism between ColTx-I and other venom components may reveal targets for the development of more specific and effective therapies.

1. Introduction

Snake venoms are libraries of pharmacologically active substances that are naturally designed to act on the specific targets of the prey or victim (Calvete, 2009; Da Silva et al., 2011), which proteins compose more than 90% of the venom dry weight, with phospholipases A_2 (PLA_2 E.C.3.1.1.4) generally being one of the most abundant (Calderon et al., 2014; Calvete, 2009). Secreted PLA_2s are stable, ubiquitous, versatile, relatively small (~14 kDa), calcium-dependent and disulfide-rich enzymes that catalyze the membrane phospholipids' hydrolysis at *sn*-2 position, generating lysophospholipids and biologically active fatty acids (Schaloske and Dennis, 2006; Van and De Haas, 1963) being usually responsible by muscle damage and playing other important toxic and digestive roles in prey capture and immobilization (Gutierrez and Ownby, 2003; Schaloske and Dennis, 2006).

Despite sharing high identity and an apparent molecular simplicity, these enzymes exert an exciting variety of pharmacological effects, which include neurotoxicity, cytotoxicity, edema-

* Corresponding author. IKIAM – Universidad Regional Amazónica, Km 7, Via Muyuna, Tena, Napo, Ecuador.
E-mail addresses: biomol2@hotmail.com, slsilva@pq.cnpq.br (S.L. Da Silva).

http://dx.doi.org/10.1016/j.toxicon.2016.03.008
0041-0101/

forming activity, bactericidal activity, myotoxicity, among others (Castillo et al., 2012; Gutierrez and Lomonte, 2013; Kini, 2003; Montecucco et al., 2008; Samel et al., 2013). The characterization of this functionally versatile group of toxins awakens medical-scientific interest due to the number of potential applications for understanding envenomation, making clinical diagnosis, developing therapeutic strategies and using these toxins as molecular and biotechnological tools in pathophysiological, taxonomic, ecological studies as well as parameters for hemostatic assays (Calderon et al., 2014; Carvalho et al., 2013; Cecilio et al., 2013; Murakami and Lambeau, 2013).

Myotoxic PLA_2s are involved in local and systemic skeletal muscle degeneration, a common pathophysiological event in viperid snakebite envenomation (Gutierrez and Ownby, 2003; Hernandez et al., 2011). These events are accompanied by an acute inflammatory reaction associated with swelling, pain and the recruitment of macrophages and polymorphonuclear leukocytes (Chacur et al., 2003; Gutierrez et al., 2009; Mamede et al., 2013). Activated leukocytes secrete a wide range of chemical mediators such as IL-1, IL-6 and IL-8, which along with the biological effects induced by the toxin, may contribute to the evolution of local myotoxicity and regeneration (Oliveira et al., 2009; Voronov et al., 1999). Local myonecrosis is a difficult medical challenge owing to its rapid development and poor tissue regeneration characterized by dysfunction and tissue loss, which have negative social and psychological consequences (Hernandez et al., 2011; Tonello et al., 2012). The effects triggered by PLA_2s occur upon interaction with lipids or proteins, altering the plasma membrane integrity by catalytically dependent or independent mechanisms that consequently mediate a number of associated events, such as: calcium influx, depolarization, loss of ionic gradients and efflux of cytosolic molecules (Kini, 2003; Montecucco et al., 2008).

The biochemical and functional characteristics of several crotalic and bothropic phospholipases have been described (Damico et al., 2008; Gutierrez and Lomonte, 2013; Higuchi et al., 2007a); however, no information is available regarding the toxic activity of purified proteins from *Crotalus oreganus lutosus,* (Great Basin rattlesnake), a venomous pitviper subspecies belonging to the Viperidae family and Western Rattlesnake complex, that is found in the Great Basin region of the United States. The Western Rattlesnakes occur across a broad geographical area and disjunct populations occur in much of the mountainous west, resulting in potential disruption of gene flow and local variation (Ashton and De Queiroz, 2001; Mackessy, 2010). Due to this, these venomous pitviper subspecies are considered an ideal species group to understand questions of what differences in venom composition occur, why these differences evolve and how composition affects the biological role of venom, as described by Mackessy (2010). In the present study, a myotoxic PLA_2 (ColTx-I) from *C. o. lutosus* was isolated and characterized in order to obtain insights into its primary structure, biological effects, induction of morphological changes of skeletal muscle and its relevance to the pathophysiology of envenomations produced by this species.

2. Material and methods

2.1. Venom and reagents

C. o. lutosus snake venom was obtained from The National Natural Toxins Research Center (NNTRC) of Texas A&M University – Kingsville (Kingsville, TX, USA). All reagents were of analytical or sequencing grade.

2.2. Animals

The male Swiss mice (18–20 g) used in this study were maintained under specific pathogen-free conditions and had free access to food and water. The animals were housed in laminar-flow cages maintained at a temperature of 22 ± 2 °C and a relative humidity of 50–60%, with a 12:12 h light–dark cycle. Animal procedures were performed in accordance with the general guidelines proposed by the Brazilian Council for Animal Experimentation (COBEA) and approved by the University's Committee for Ethics in Animal Experimentation (CEEA/UNICAMP), number 3245-1.

2.3. Isolation of ColTx-I from C. o. lutosus snake venom

One hundred mg of *C. o. lutosus* snake venom were dissolved in 1 ml of ammonium bicarbonate buffer (0.2 M, pH 7.8), homogenized until reaching complete dissolution and centrifuged at 5000 × g (5 min). The supernatant obtained was loaded onto a Sephadex G75 column (1.5 cm × 90 cm, Amersham Pharmacia Biotech), previously equilibrated with ammonium bicarbonate buffer (50 mM, pH 7.8) and run at a flow rate of 0.2 ml/min. Three peaks were obtained (Col-I, Col-II and Col-III – Fig. 1A), which were lyophilized and stored at − 20 °C. Subsequently, 5 mg from the lyophilized fraction of Col-II, which showed PLA_2 activity (Fig. 1A), were dissolved in 120 μl of 0.1% (v/v) trifluoroacetic acid (solvent A) and 80 μl of 1 M ammonium bicarbonate. The resulting solution was centrifuged at 5000 × g (2 min) and the supernatant was submitted to reverse-phase chromatography (Waters 991-PDA system) using an analytical C18 column (Supelco, 250 mm × 4.6 mm). The C18 column was equilibrated in solvent A and the elution proceeded with a concentration gradient from 0 to 100% of solvent B (66% acetonitrile, 0.1% TFA), at a flow rate of 1 ml/min (60 min). The elution profile of both chromatography analyses was monitored at 280 nm, and the collected fractions of 3 ml were lyophilized and stored at −20 °C. All peaks (Fig. 1B) were tested for PLA_2 activity and the active peak was named ColTx-I (Fig. 1B). This peak was re-chromatographed (Fig. 1C) to evaluate its purity, under the same conditions as described above (RP-HPLC) and was further biochemically and functionally characterized.

2.4. Electrophoresis

The relative molecular mass of ColTx-I and homogeneity was evaluated using sodium dodecyl sulfate polyacrylamide gel electrophoresis (SDS-PAGE), according to the method described by Laemmli (1970). Samples were heated at 100 °C (5 min) and then run under reducing and non-reducing conditions (Vargas et al., 2012; Vieira et al., 2013).

2.5. Phospholipase A_2 activity

PLA_2 activity was measured using a non-micelar substrate, 4-nitro-3-octanoyloxy benzoic acid (NOBA), according to the assay method described by Cho and Kezdy (1991) and Holzer and Mackessy (1996) adapted for 96-well plates (Calgarotto et al., 2008; Damico et al., 2005). The PLA_2 activity, expressed as the initial velocity of the reaction (V_o), was calculated based on the increase in absorbance at 425 nm after 20 min. The effects of pH, temperature, substrate concentration and divalent ions on PLA_2 activity were also investigated.

2.6. MALDI-TOF mass spectrometry analysis of ColTx-I

The molecular mass of ColTx-I was determined by matrix-assisted laser desorption/ionization-time-of-flight (MALDI-TOF)

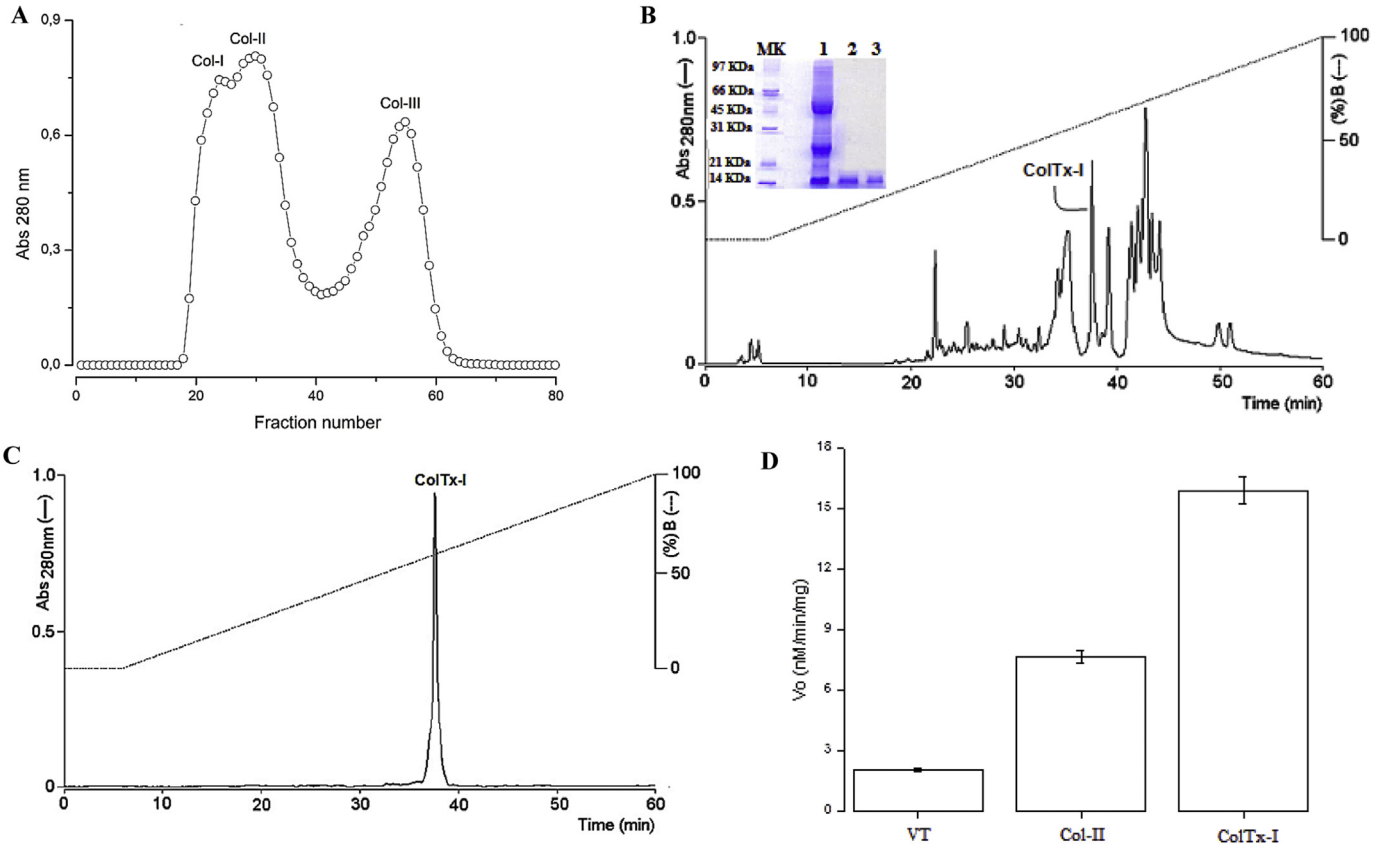

Fig. 1. Sequential purification steps of ColTx-I. (A) Elution profile of *Crotalus oreganus lutosus* by molecular exclusion chromatography on a Sephadex G-75 column (Amersham Pharmacia Biotech, 1.5 cm × 90 cm) using 50 mM ammonium bicarbonate buffer; pH 8.0 at flow rate of 0.2 ml/min. (B) Profile elution of Col-II by RP-HPLC on an analytical C18 column (Supelco, 250 mm × 4.6 mm). The peak corresponding to ColTx-I is indicated. Insert: Electrophoretic analysis in SDS-PAGE (12%). Lines: (MK) molecular mass markers (1) ColTx-I reduced and (2) not reduced. (C) Rechromatography of ColTx-I on a RP-HPLC C18 column. (D) The PLA_2 activity was monitored during the purification procedure. PLA_2 activity of *C. o. lutosus* venom (**VT** – **1 μg/μl**), Col-II (size exclusion – **1 μg/μl**) and ColTx-I (RP-HPLC – **1 μg/μl**).

mass spectrometry using a MALDI-TOF/TOF – Proteomics Analyzer 4700 (AB SCIEX). ColTx-I was dissolved in a solution of 50% acetonitrile/high purity water (ACN/H2O; v/v) and 1 μl of matrix (10 mg/ml α-Cyano-4-hydroxycinnamic acid in 50% ACN/H_2O (v/v), 0.1% trifluoroacetic acid) was mixed with 1 μl of the sample on the MALDI plate. The instrument was calibrated using a BSA standard solution and analyzed under the same conditions (Martins et al., 2014). Mass values given correspond to m/z of the centroid of the envelope of the mass peaks for protonated molecular ions $[M+H]^+$.

2.7. N-terminal sequencing

In order to obtain N-terminal sequence of ColTx-I, approximately 50 μg of this toxin was submitted for amino terminal amino acid sequencing using the automated Edman degradation method (Edman, 1950) on a PPSQ-33A (Shimadzu) automatic sequencer (Martins et al., 2014).

2.8. Sequencing procedure

2.8.1. In solution digestion

ColTx-I was reduced with dithiothreitol, alkylated with iodine acetamide and digested overnight at 37 °C with trypsin and LysC (Sequencing grade modified, Promega) – independent experiments. Proteolytic fragments were dried in a vacuum centrifuge and **redissolved** in 1% formic acid for LC–MS/MS analysis.

2.8.2. LC–MS/MS analysis and database search

Protein identification was carried out in a NanoAcquity (Waters) UPLC coupled with an Orbitrap Velos mass spectrometer (Thermo Scientific). An aliquot of the tryptic digest was separated in a C18 reverse phase column [75 μm Øi (internal diameter), 10 cm, NanoAcquity, 1.7 μm BEH column, Waters], according to the conditions described by Martins et al. (2014). Raw data were analyzed using Proteome Discoverer (v.1.3.0.339) software and run with the search engine MASCOT against NCBInr Serpentes database. Only high confidence peptides (FDR≤ 0.05) were considered for identification results (Martins et al., 2014).

2.9. Alignment and phylogenetic study

The amino acid sequences of toxins used for multiple sequence alignment and phylogenetic three reconstruction were obtained from NCBI (National Center for Biotechnology Information) database using the BLASTP (Protein Basic Local Alignment Search Tool) algorithm and BLOSUM62 substitution matrix. Due to few sequences of basic Asp49 PLA_2s available and published from venoms of species belongs to Western Rattlesnake Complex, were selected toxins sequences of six different Genus with similarity to ColTx-I structure primary. The minimum e-value showed by the selected sequences used in these analyses was $2 \times e^{-55}$. The multiple sequence alignment was performed with CLUSTAL W (1.8), while the phylogenetic tree was inferred using the neighbor-joining method (Saitou and Nei, 1987) implemented in a computer program.

2.10. Local and systemic myotoxicity

Two separate groups of six male Swiss mice (18–20 g) were used in myotoxicity studies. One group received an intramuscular injection in their right gastrocnemius muscle (local myotoxicity), while another received an intravenous injection (systemic myotoxicity) of variable amounts of ColTx-I (5, 10 and 20 μg/mice) dissolved in 50 μl of PBS (120 mM NaCl, 40 mM NaH_2PO_4, pH 7.2). Control groups received an identical intramuscular or intravenous injection of PBS alone. At different time intervals (before, 1, 3, 6, 9 and 24 h after injection), a tail blood sample was collected into heparinized capillary tubes, centrifuged and a plasma aliquot was utilized to determine the creatine kinase activity using a kinetic assay (CK-Nac Bioliquid). The assay results were obtained using VersaMax™ ELISA Microplate Reader. Enzyme activity was expressed in U/L, where one unit corresponds to the production of 1 mmol of NADH min^{-1} at 25 °C.

2.11. Histological evaluation

Myotoxic activity was also investigated on the basis of morphological alterations caused by injection of 20 μg/mice of ColTx-I in the right gastrocnemius skeletal muscle of groups of six male Swiss mice (18–20 g). Control animals received an injection of PBS alone. One hour after the injection the animals were sacrificed by an overdose of ketamine/xylazine and a central region of the muscle was removed. The excised material was then soaked in fixing solution (10% formaldehyde in PBS, v/v), dehydrated in ascending ethanol concentrations and processed for inclusion in paraffin. The resulting blocks were sliced into 6.0 mm thick sections, stained with Hematoxylin and Eosin and examined under a light microscope (Mamede et al., 2013).

2.12. Edema-forming activity

The ability of ColTx-I to induce edema was studied in groups of six Swiss mice (18–20 g). Fifty μl of PBS with ColTx-I (5, 10, 20 μg/paw) were injected in the subplantar region of the right footpad. As a control, 50 μl of PBS were injected in the left footpad. The paw volume was measured with a low-pressure pachymeter (Mitutoyo, Japan) before and at various intervals after injection (0.5, 1, 3, 6, 9 and 24 h) (Vieira et al., 2013). Edema-inducing activity was expressed as the percent increase in volume of the right footpad, relative to the reading obtained in the left footpad (control) at each time interval after and before the injection and calculated using the following formula: % edema = [(Tt × 100)/To) − 100], where Tt corresponds to edema (volume) measured at each time interval induced by ColTx-I and To is the paw volume at the initial time (intact paw, before injection). The percentage of edema calculated was subtracted from the matched values at each time point in the PBS-injected left paw (control).

2.13. Interleukin-6 (IL-6) measurement

Groups of six Swiss mice (18–20 g) received an injection of 5, 10 or 20 μg/50 μl of ColTx-I in the tibialis anterior muscle. A control group received an injection of PBS (50 μl) under the same conditions. Tail blood samples were collected into heparinized capillaries at different time intervals (0.5, 1, 3, 6, 9, 12 and 24 h after toxin injection) and the plasma was removed for quantitative determination of interleukin-6 (IL-6) levels through an enzyme-linked immunosorbent assay (Mouse IL-6 ELISA Set BD Biosciences) (Calgarotto et al., 2008).

2.14. Statistical analysis

Results were expressed as means ± standard deviations (SD) obtained with the indicated number of assays. Statistical significance of differences between groups was evaluated by ANOVA or Kruskal–Wallis tests and confirmed by Tukey and Tukey-type tests. Differences were considered statistically significant if $p < 0.05$.

3. Results

3.1. Isolation of ColTx-I

The ColTx-I myotoxin was isolated from *C. o. lutosus* snake venom through a combination of two chromatographic steps: gel filtration (size exclusion) and reverse-phase high-performance liquid chromatography (Fig. 1A and B, respectively). The crude venom was fractionated into three major fractions, named Col-I, Col-II and Col-III (Fig. 1A), by size exclusion chromatography on a Sephadex G-75 column. PLA_2 assays of all fractions revealed the high PLA_2 activity of Col-II. The Col-II fraction was dissolved and purified using reverse-phase HPLC on a C18 column, resulting in the chromatographic profile shown in Fig. 1B. All peaks were analyzed for PLA_2 activity. The fraction detached in Fig. 2B named as ColTx-I showed high phospholipase activity and was selected for biochemical and functional characterization.

The course of protein purification was accompanied by an increase in specific activity (Fig. 1D). ColTx-I showed higher PLA_2 activity when compared to Col-II and crude venom (Fig. 1D). The homogeneity and purity of ColTx-I were confirmed by rechromatography on an analytical C18 column (Supelco), showing the presence of a well-resolved sharp peak (Fig. 1C), and by SDS-PAGE, which revealed a single band of ≅14 kDa under reducing and non-reducing conditions (Fig. 1B insert).

3.2. Primary structure analysis of ColTx-I

Both the homogeneity and molecular mass of ColTx-I were determined by MALDI–TOF mass spectrometry analysis, which showed sharp peaks at a m/z value of 7072 double charged ions (where z = +2), and a m/z of 14,146 for mono charged ions (where z = +1) (Fig. 2). The calculated molecular mass weight (Mw) of this PLA_2 was14,145 Da and was calculated by averaging of the (Mw) between the protein in states (+1) and (+2).

The complete sequence of ColTx-I (HLLQFNKMIKFETRKNAIPFYAFYGCYCGWGGRGRPKDATDRCCFVHDCCYGKLTDCSPKWDIYPYSLKSGYITCGKGTRCEKQICECDRVAAECLRRSLSTYKYGYMFYPDSRCKGPSEQC) is showed in Fig. 3A, and the theoretical molecular mass for this sequence is 14,043 Da and its very closed to the calculated molecular mass weight (14,145 Da) which was calculated by averaging of the (Mw) between the protein in states (+1) and (+2) (Fig. 2). The complete sequence of this protein was archived in UniProt Knowledge base, regarding SPIN ID number SPIN200006353 (provisorial).

In order to perform the molecular identification and homology study, purified ColTx-I was submitted for amino terminal amino acid sequencing and digested with trypsin and Lys C for analysis by LC/MS/MS. The following N-terminal sequence: HLLQFNKMIKFETRKNAIPFYAFYGCYCGWGGRGRPKDATDRCCFVH was obtained by Edman degradation. Twenty peptides were identified by LC/MS/MS (Tables 1 and 2), which allowed for complete primary structure determination and classification of the protein as an Asp49-PLA_2 (fragment 4 – DATDRCCFV**HD**CCYGK – active site – Table 1), consistent with enzymatic assays which demonstrated the ability of ColTx-I to hydrolyze the chromogenic substrate. ColTx-I shares functional motifs with group II PLA_2s, including the calcium-

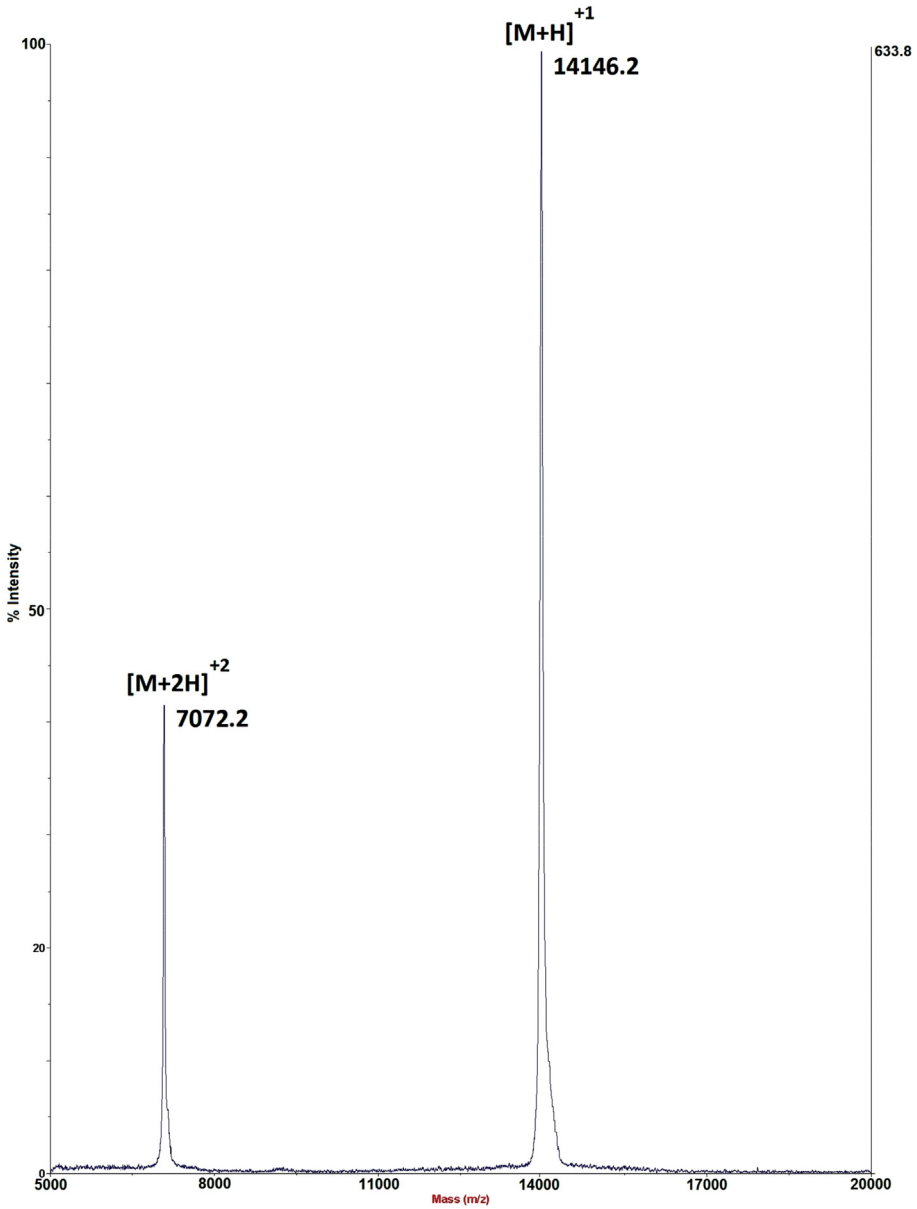

Fig. 2. MALDI-TOF MS analysis of ColTx-I. The spectrum demonstrates the mass/charge ratio (*m*/*z*) of ColTx-I determined by matrix-assisted laser desorption/ionization-time-of-flight using a MALDI-TOF/TOF – Proteomics Analyzer 4700 (AB SCIEX) demonstrating a Mw of 14,146 Da to Mw in state (+1) and a Mw 7.072 Da to Mw in state (+2). The final Mw is 14,145 Da and was calculated by averaging between the protein in states (+1) and (+2).

binding site (fragment 3- KNAIPFYAFYGCYCGWGGR – Table 1), the active site and the N-terminal region (fragment 1 – HLLQFNK – Table 1). ColTx-I showed a high content of Lys, Arg and Tyr residues typical of a basic PLA_2.

A comparison of the partial amino acid sequence of ColTx-I with similar proteins in the database showed that its primary structure is closely related to that of viperid basic PLA_2s (Fig. 3A). The amino acid sequence analysis revealed that ColTx-I has a strong evolutionary relationship with T1DE90, a basic PLA_2 from *Crotalus oreganus helleri* (pI = 8.84) (Fig. 3B).

3.3. Biochemical and pharmacological characterization

The effect of the substrate on the PLA_2 activity of ColTx-I is shown in Fig. 4A. The kinetic parameters K*m* and Vmax were determined to be 8.09 mM and 15.97 nmol/min/mg, respectively. As expected, maximum enzymatic activity occurred at 37 °C (Fig. 4B) and the optimal pH was 8.0 (Fig. 4C). Furthermore, the enzymatic analysis demonstrated that Ca^{2+} is an essential cation for the PLA_2 activity of the purified toxin. ColTx-I showed low activity when the enzymatic assay was performed using only the Tris–HCl buffer (pH 8.0) with no added calcium. In the presence of chelating agents EDTA and EGTA, no significant PLA_2 activity of ColTx-I was detected, whereas the addition of calcium to the buffer was enough to achieve maximum activity (Fig. 4D). In contrast to Ca^{2+}, none of the other tested ions (Cd^{2+}, Mg^{2+}, Mn^{2+}, Zn^{2+}) activated the purified toxin. The obtained data clearly show that the substitution of Ca^{2+} for other divalent ions significantly reduces the catalytic activity of ColTx-I. Interestingly, Mg^{2+} and Mn^{2+}, in the presence of 10 mM Ca^{2+}, were found to support a significant phospholipase activity, while notable inhibition of enzymatic activity was observed for Cd^{2+} and Zn^{2+}, even in the presence of

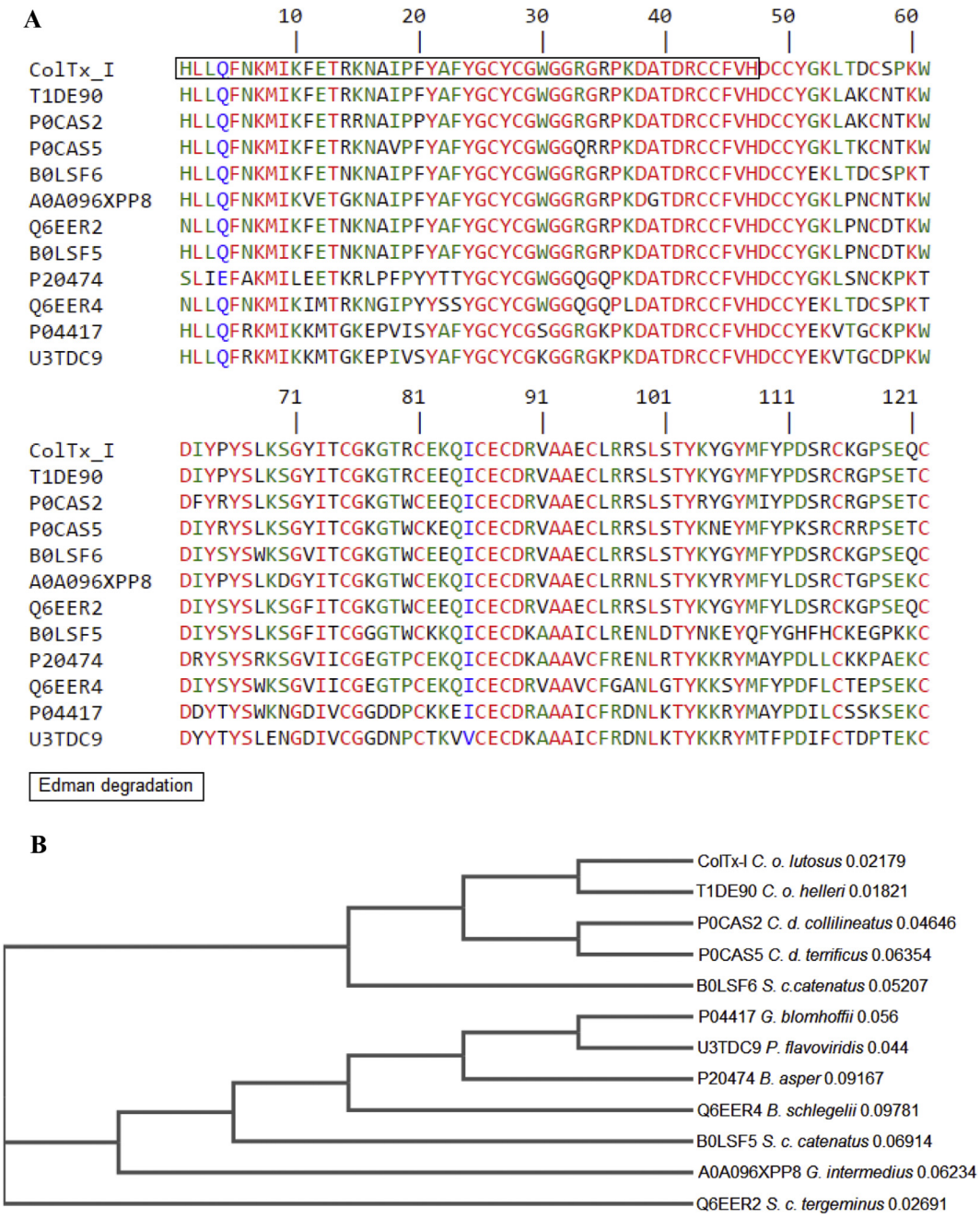

Fig. 3. Multiple sequence alignment of ColTx-I with related proteins in viperid snake venoms and their phylogeny relationship. (A) Protein codes correspond to the UniProtKB database at ExPAsy Proteomics Serve or PDB. T1DE90: basic PLA_2 from *Crotalus oreganus helleri* (pI = 8.84) (Sunagar et al., 2014), P0CAS2: basic PLA_2 from *Crotalus durissus collilineatus* (pI = 8.85) (Salvador et al., 2009), P0CAS5: basic PLA_2 from *Crotalus durissus terrificus* (pI = 9.16) (Toyama et al., 2003), Q6EER2: basic PLA_2 from *Sistrurus catenatus tergeminus* (pI = 8.37) (Chen et al., 2004), P20474: basic PLA_2 from *Bothrops asper* (pI = 8.72) (Kaiser et al., 1990), U3TDC9: basic PLA_2 from *Protobothrops flavoviridis* (pI = 8.36) (Aird et al., 2013), P04417: basic PLA_2 from *Gloydius blomhoffii* (pI = 8.71) (Forst et al., 1986), Q6EER4: PLA_2 from *Bothriechis schlegelii* (pI = 6.69) (Chen et al., 2004), A0A096XPP8: basic PLA_2 from *Gloydius intermedius* (pI = 8.73) (Yang et al., 2015), B0LSF6: basic PLA_2 from *Sistrurus catenatus catenatus* (pI = 8.19) (Gibbs and Rossiter, 2008) and B0LSF5: basic PLA_2 from *Sistrurus catenatus catenatus* (pI = 8.62) (Gibbs and Rossiter, 2008). (B) Evolutionary relationship of ColTx-I with other PLA_2 isoforms based on the final alignment.

10 mM Ca^{2+} (Fig. 4D).

In order to identify possible functional roles and to understand the molecular and pathophysiological mechanism of action of envenoming by *C. oreganus lutosus*, an evaluation of *in vivo* pharmacological/toxic activities induced by ColTx-I was performed. The purified toxin is a potential myotoxic factor in *C. o. lutosus* venom. The results shown in Fig. 5A and B demonstrate that ColTx-I induced both local and systemic myotoxicity. Intramuscular injection of increasing doses of ColTx-I triggered a rapid onset and dose-dependent elevation of plasma creatine kinase activity, which reached maximum levels 1 h after i.m. injection and returned to basal levels within 24 h (Fig. 5A). Intravenous injection of the purified toxin also resulted in a prominent increase in plasma CK activity as compared to the PBS control group. Fig. 5B shows that, *in vivo*, ColTx-I induced systemic myotoxic effects quickly, reaching the highest levels 1 h after i.v. injection, when a dose of 20 μg was administered. However, ColTx-I promoted a higher release of CK when injected into the gastrocnemius muscle compared to the

Table 1
Tryptic peptides fragments of ColTx-I obtained by LC–MS/MS sequencing. The isolated myotoxin was reduced, alkylated and digested overnight with trypsin. Eluted tryptic peptides were dried in a vacuum centrifuge and **redissolved** in 1% formic acid for LC–MS/MS analysis.

Number	Peptide fragment	Molecular mass (Da)		Accuracy (ppm)
		Monoisotopic	Theoretical[b]	
1	HLLQFNK[a]	898.5012	898.5025	1.4
2	MIKFETRK[a]	923.4887	923.4899	1.3
3	KNAIPFYAFYGCYCGWGGR	2286.0128	2286.0139	0.8
4	DATDRCCFVHDCCYGK	2062.7826	2062.7754	−3.5
6	LTDCSPK	820.3869	820.3889	−2.4
7	WDIYPYSLK	1183.5907	1183.5913	0.5
8	SGYITCGK	885.4123	885.4125	−2.0
9	QJCECDR	980.3928	980.3931	−0.3
10	VAAECLRR	973.5197	973.5127	−7.2
11	SLSTYK	853.4740	853.4657	−9.7
12	YGYMFYPDSR	1297.5281	1297.5437	12.0
13	CKGPSEQC	964.3723	964.4803	112.0

[a] Confirmed by Edman sequencing.
[b] Cysteine and methionine residues are changed into carbamidomethyl and oxidized methionine, respectively.

Table 2
Lys C peptide fragments of ColTx-I obtained by LC–MS/MS sequencing. The isolated myotoxin was reduced, alkylated and digested overnight with Lys C. Eluted peptides were dried in a vacuum centrifuge and **redissolved** in 1% formic acid for LC–MS/MS analysis.

Number	Peptide fragment	Molecular Mass (Da)		Accuracy (ppm)
		Monoisotopic	Theoretical[b]	
1	HLLQFNK[a]	899.5106	899.5102	0.4
2	DATDRCCFVHDCCYGK	2062.7654	2062.7599	2.6
3	LTDCSPK	820.3869	820.3881	−1.5
4	WDIYPYSLK	1184.6025	1184.5998	2.3
5	SGYITCGK	885.4133	885.4136	−0.3
6	GTRCEK	750.3563	750.3568	−0.7
7	YGYMFYPDSRCK	1600.6923	1600.6918	0.3

[a] Confirmed by Edman sequencing.
[b] Cysteine and methionine residues are changed into carbamidomethyl and oxidized methionine, respectively.

intravenous injection.

Histological analyses confirmed the high levels of CK liberated by the gastrocnemius muscle. Histological evaluation by light microscopy showed important morphological alterations in the muscle provoked by ColTx-I, when compared to the control group (Fig. 6). The myotoxic effect induced by ColTx-I, was characterized by drastic cellular destruction (necrosis – Fig. 6B, D, E and F), edema (Fig. 6E) and abundant inflammatory infiltrate cells, constituted predominantly by neutrophils (Fig. 6D and E).

Subplantar injection of ColTx-I induced mice paw edema, indicating an increase in vascular permeability at the inoculation site of the toxin. The dose-dependent local edema induced by ColTx-I displays a similar time–course profile, characterized by rapid onset; maximal responses were obtained 30 min post-injection (Fig. 7).

The analysis of mechanisms behind the inflammatory reactions caused by ColTx-I showed a marked increase in proinflammatory cytokine Interleukin-6 (IL-6) levels, reaching a maximum increase 1 h after injection, when compared with the control (Fig. 8).

4. Discussion

Due to their functional versatility and role in myotoxicity, many studies have researched compounds to aid in the treatment of snakebites to inhibit the toxic effects of PLA_2, as well as to isolate and characterize new PLA_2s (Carvalho et al., 2013; Da Silva et al., 2009; Da Silva et al., 2008; Terra et al., 2015). The combination of two chromatographic steps: size exclusion and RP-HPLC, widely used for purification of PLA_2s (Damico et al., 2005, 2012; Martins et al., 2014), effectively isolated ColTx-I. The molecular homogeneity assessed by SDS-PAGE, under reducing and non-reducing conditions, revealed the presence of a single band with an apparent MM of 14 kDa, consistent with the molecular mass determined by mass spectrometry (14,145 Da), and evidenced its monomeric nature and lack of tendency to form aggregates, a common feature of other snake venoms PLA_2s, which also consist of a single polypeptide chain (Fig. 1A–D) (Damico et al., 2005; Fernandez et al., 2010; Higuchi et al., 2007b).

The amino acid composition of ColTx-I revealed a highly basic and hydrophobic content and 14 cysteine residues, similar to other basic PLA_2 myotoxins (Damico et al., 2005; Romero et al., 2010). The presence of these cysteine residues suggests the presence of 7 disulfide bonds, a common structural characteristic of PLA_2s, which are important for stabilizing the three-dimensional structure (Kini, 2003; Schaloske and Dennis, 2006), while the high content of basic and hydrophobic residues probably indicates the interaction of the toxin with target sites, mediating the toxic effects (Kini and Evans, 1989; Murakami and Arni, 2003). The cellular target and pharmacological sites (structural determinants of biological activities presents in primary structure of toxin) should be complementary to each other in terms of van der Waal's contact surfaces, charges and hydrophobicity and (Kini, 2003). Several studies have showed and suggested that the hydrophobic and positively charged patch on the surface of PLA_2s plays an essential role in myotoxic activity (Murakami and Arni, 2003; Murakami et al., 2005; Zhou et al., 2008).

ColTx-I exhibits well-conserved functional motifs, such as the calcium-binding site, catalytic site and N-terminal region (Table 1), which retain a high degree of similarity among group II PLA_2s (Schaloske and Dennis, 2006), particularly among the basic PLA_2s

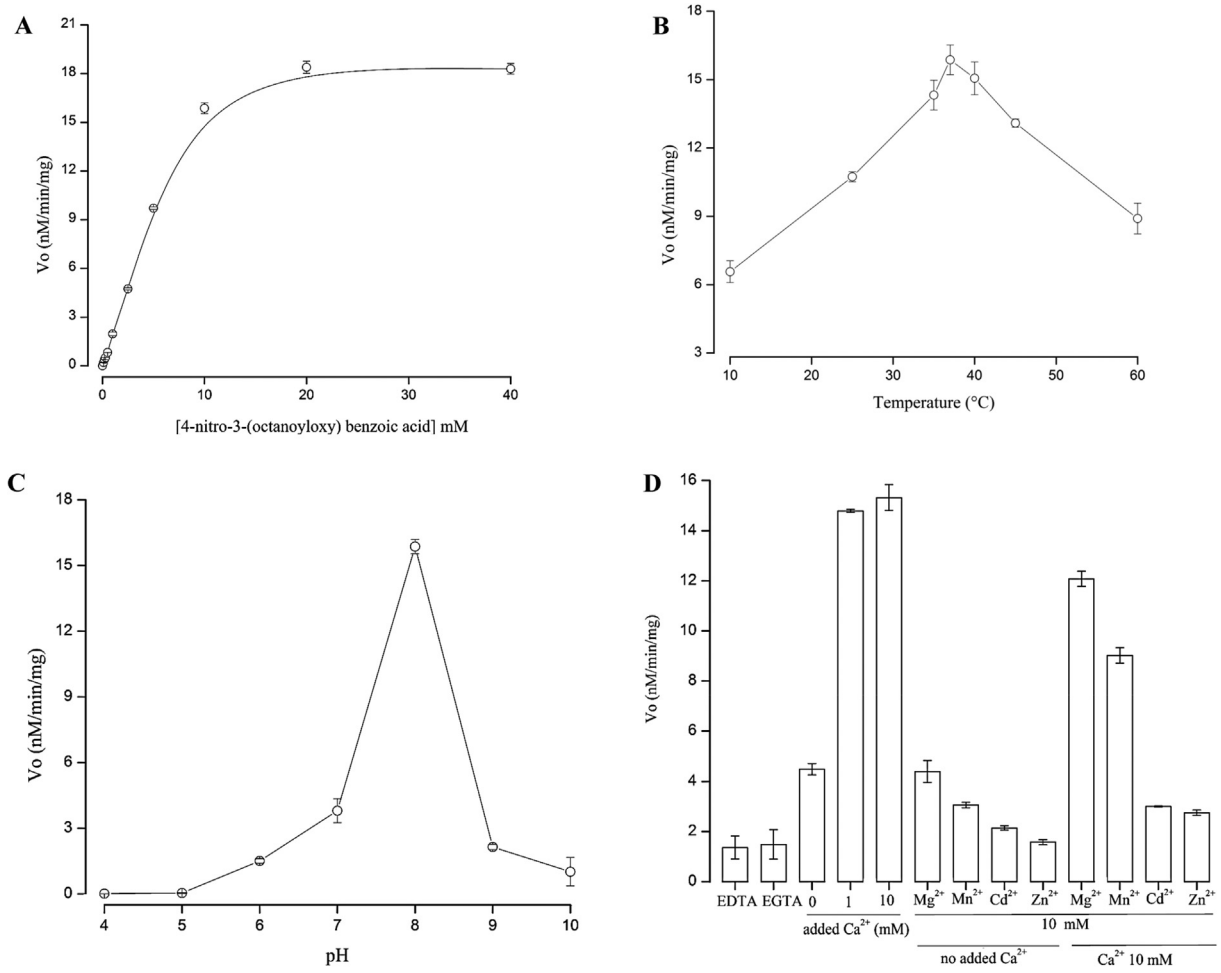

Fig. 4. Enzymatic characterization of ColTx-I. (A) Effect of substrate concentration on the PLA_2 activity of ColTx-I. (B) Effect of temperature on the PLA_2 activity of ColTx-I. (C) Evaluation of PLA_2 activity of ColTx-I at different pH values. (D) Influence of metal ions and chelating agents on ColTx-I activity. All enzymatic assays were conducted using the non-micelar substrate, NOBA. Results are expressed as means ± SDs of three independent experiments performed in triplicate.

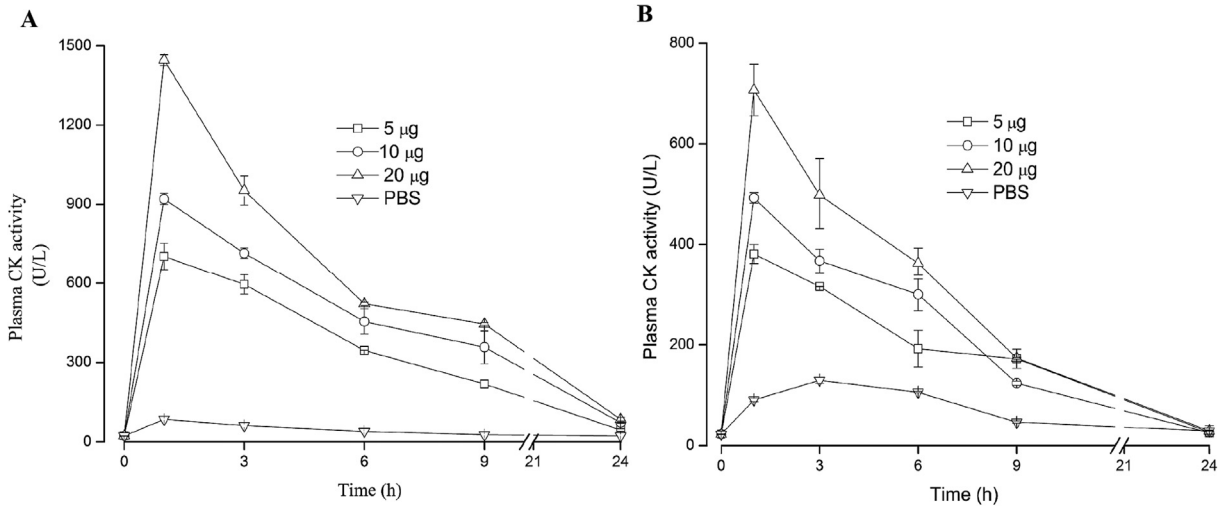

Fig. 5. Myotoxic activity induced by ColTx-I from *Crotalus oreganus lutosus*. (A) Time-course of the increase in plasma CK activity after intramuscular injection and (B) intravenous injection of ColTx-I (5, 10 and 20 µg/animal). Controls were injected with 50 µl of PBS. At different times (0, 1, 3, 6, 9 and 24 h), tail blood samples were collected and plasma creatine kinase activity was determined using a kinetic assay. Myotoxic activity was expressed as mean ± SD of three independent experiments performed in triplicate (n = 6).

from viperid venoms (Bouchier et al., 1988; Chen et al., 2004; Damico et al., 2005; Diz Filho et al., 2009; Faure et al., 2011) (Fig,

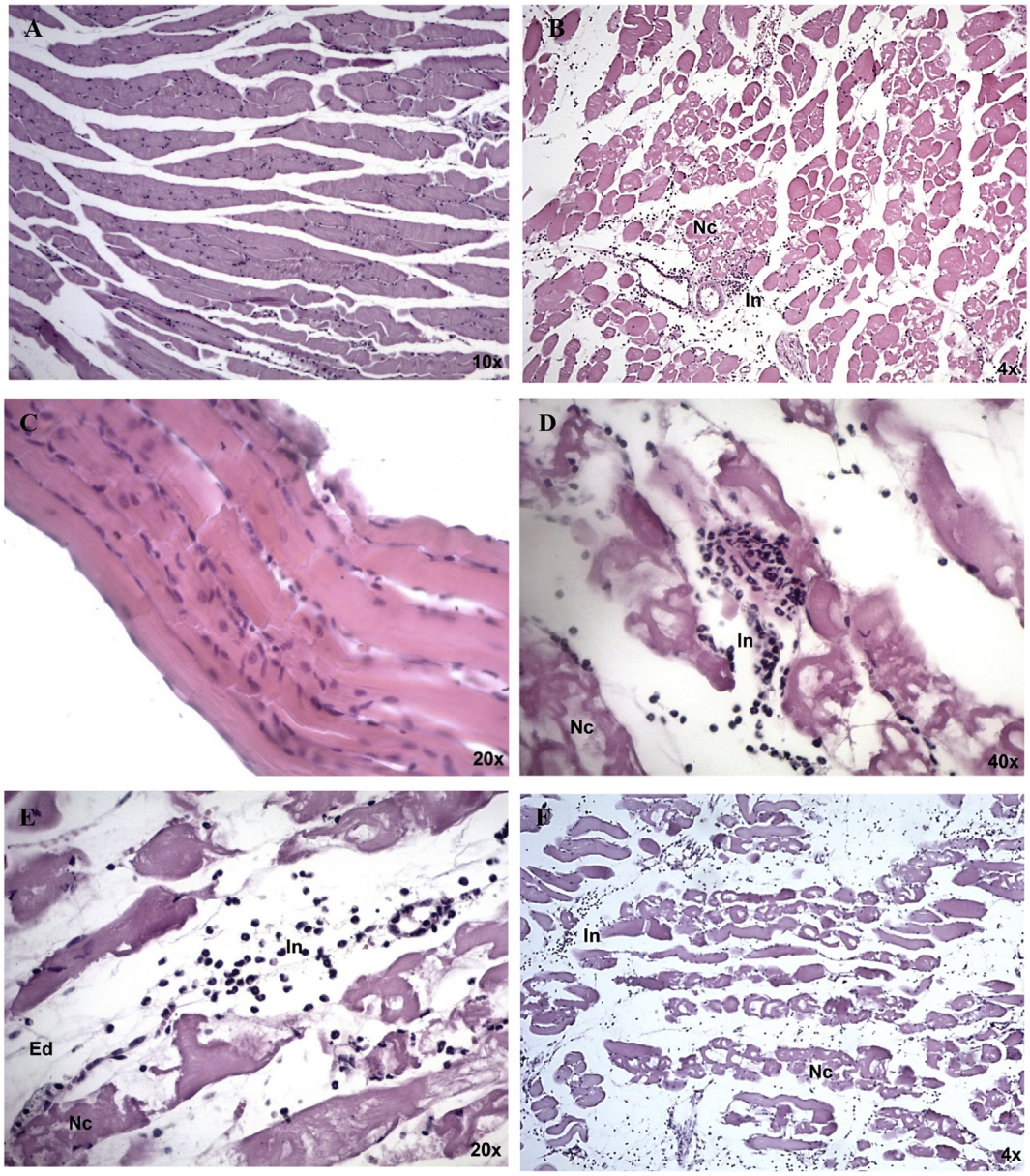

Fig. 6. Histological alterations of muscle damage induced by ColTx-I. Light micrographs of sections from the right mice gastrocnemius muscle 1 h after the injection of 20 μg/animal of isolated myotoxin from *Crotalus oreganus lutosus*, dissolved in 50 μl PBS, stained with hematoxylin–eosin. (A, C) Control mice were injected with PBS alone: normal integral fibers are observed. (B, D, E and F) Muscle sections of mice injected with the isolated myotoxin showing edema (Ed), necrosis (Nc) and inflammatory infiltrate (In).

3). The calcium-binding site identified in the ColTx-I sequence contains four glycine residues (G25, G29, G31 and G32), which has been related to the flexibility of the loop that allows for the coordination of calcium for catalytic activity (Chang et al., 1997).

In order to provide more insight into the kinetic behavior of ColTx-I, this was evaluated using the synthetic chromogenic substrate, NOBA (Damico et al., 2012; Martins et al., 2014). Vmax and Km were calculated to be 15.97 nmol/min and 8.09 mM, respectively. Maximum PLA_2 activity of ColTx-I occurs at pH 8 and 37 °C (Fig. 4A–C). LmTX-I isolated from *Lachesis muta* muta (Damico et al., 2005) and BmTX-I from *Bothrops moojeni* (Calgarotto et al., 2008) display thermal stability and an optimum pH similar to ColTx-I using the same substrate.

Studies have provided strong evidence that the divalent cation, Ca^{2+}, is essential for both catalytic activity and PLA_2 binding to the substrate (Damico et al., 2005; Yu et al., 1998). The PLA_2 activity of ColTx-I in the presence of chelating agents was significantly inhibited, similar to the inhibition observed when Ca^{2+} was replaced by divalent cations, which were not able to maintain the enzymatic activity of ColTx-I. However, when calcium ions were added, the purified enzyme presented PLA_2 activity, as seen in enzymatic assays for other PLA_2s of the *Bothrops* and *Crotalus* genus, using the same substrate (Calgarotto et al., 2008; Martins et al., 2014). Evidence has shown that the role of the calcium ion is crucial not only for the electrophilic behavior of the catalytic site, but also for the stabilization of the flexible Ca^{2+}-binding loop, to optimize the protein conformation for interactions with the substrate (Mezna et al., 1994; Yu et al., 1998). Others cations with valences of +2 (Fig. 4D) failed to allow enzyme–substrate interaction, competitively inhibited calcium-mediated activity, or proved to be weakly active, probably because of their sizes and numbers of electron shells (Mezna et al., 1994).

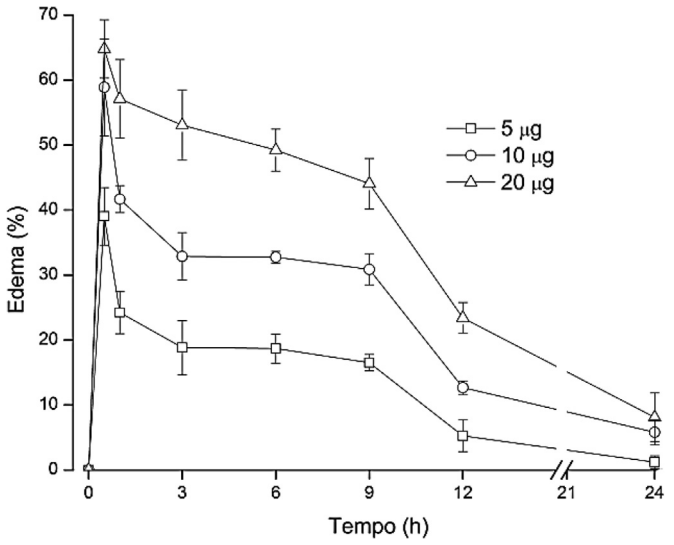

Fig. 7. Dose-dependent mice paw edema provoked by ColTx-I. Footpad thickness was determined before, and at different times after, the injection of ColTx-I (5, 10 and 20 µg/animal) and edema was calculated as the percent increase in volume of the right footpad relative to the reading obtained in the left footpad (control) at each time interval and before the injection. The edema-inducing percentage is expressed as the mean ± SD of three independent experiments performed in triplicate (n = 6).

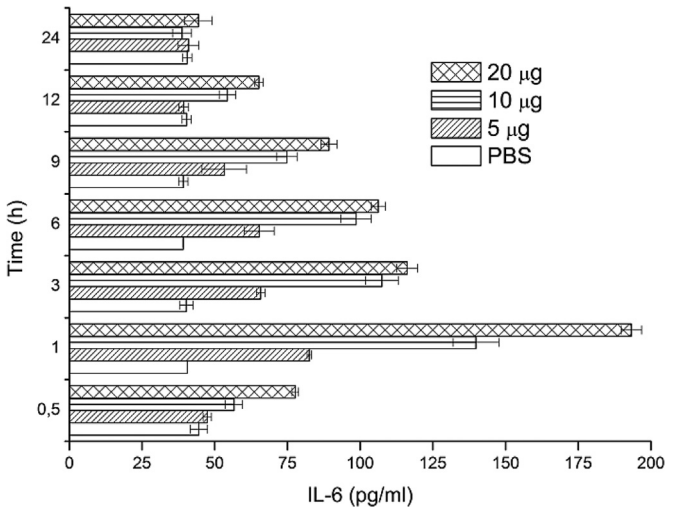

Fig. 8. Systemic interleukin-6 response triggered by different doses of ColTx-I. IL-6 plasma levels were determined at the indicated time points, by an enzyme immunoassay and expressed as the mean ± SD of three independent experiments performed in triplicate (n = 6).

ColTx-I, a typical PLA_2-D49, elicited both local and systemic myotoxic activity, owing to its high selectivity for targets in muscle cells and the ability to act on anatomical sites distant from the inoculation site (Fig. 5 and B). Some studies have shown that acidic PLA_2s (D49), although enzymatically active, are not capable of promoting muscle damage (Fernandez et al., 2010; Silveira et al., 2013; Vargas et al., 2012) and that despite their lack of enzymatic activity, Lys49-PLA_2 homologs cause severe myonecrosis (Tonello et al., 2012). These studies have suggested that pharmacologic effect depends not only on phospholipid hydrolysis, but is also closely associated with the precise site and model of binding of PLA_2 to the cell acceptors, which plays a decisive role in the location, extent of tissue damage and consequently the clinical and toxicological profile (Kini, 2003; Montecucco et al., 2008). Intramuscular injection of ColTx-I triggered greater CK levels than its intravenous injection, which may occur due to accessibility of toxins to muscles and/or toxin sequestration by binding to low-affinity sites in the membranes of other cell types (Kini, 2003; Kini and Evans, 1989; Montecucco et al., 2008). These data are consistent with the model proposed by Kini and Evans to explain the pharmacological profile of venom PLA_2s; after entering the blood, the toxin remains in the circulation until it reaches a particular organ or tissue because of its high affinity for that target (Kini, 2003; Kini and Evans, 1989). The ability to promote necrosis in muscles located in the vicinity of the injection site, as well as to reach and act on distant anatomical loci has been described for a number of PLA_2 myotoxins from the *Crotalus* genus (Gutierrez and Ownby, 2003; Montecucco et al., 2008). In contrast to crotalic PLA_2s, bothropic myotoxins induce muscle damage mainly limited to the injection site, with very little systemic myotoxicity (Gutierrez and Ownby, 2003). Systemic myotoxins cause significant increments in plasma CK activity, the breakdown of muscle fibers and myoglobinuria (Ponraj and Gopalakrishnakone, 1996). The dichotomy between local and systemic myotoxic activity establishes a clinical correlation, since *Crotalus* envenomations are characterized by the induction of local and systemic effects, such as acute renal failure (Gutierrez et al., 2009; Montecucco et al., 2008).

Histopathological analysis of local tissue damage induced by ColTx-I evidenced extensive cellular destruction, edema and leukocyte infiltrate (Fig. 6A–E). Experimental studies of the effects triggered by PLA_2, such as the myotoxin from *Bothrops alternatus* (Mamede et al., 2013), BnSP-7 from *B. (neuwiedi) pauloensis* (Oliveira et al., 2009) and LmTX-I from *L. muta* muta (Damico et al., 2008), on skeletal muscle revealed similar morphological alterations. The infiltration of inflammatory cells, mainly neutrophils accumulating in the affected tissues within the first hours of toxin injection is a typical consequence of acute local pathology (Gutierrez et al., 2009). Studies have indicated that neutrophils contribute to the muscle regenerative response, probably by removing necrotic debris and providing inflammatory messengers, such as IL-6 (Tecchio and Cassatella, 2014; Teixeira et al., 2003; Zimmermann et al., 2015).

Local inflammation has often been related to pathological effects in viperid snake envenomation (Gutierrez et al., 2009). Similarly, Bl-PLA_2 isolated from *Bothrops leucurus* (Nunes et al., 2011), a PLA_2 from *C. oreganus abyssus* (Martins et al., 2014), and ColTx-I were able to induce local inflammatory responses reaching maximum values in the first 30 min. Basic biochemical mechanisms behind paw edema mainly involve phospholipid hydrolysis with subsequent release of biologically active fatty acids and platelet activating factor or mast cell histamine release (Teixeira et al., 2009) and/or the interaction of the pharmacological domain, independently of the catalytic site (Zuliani et al., 2005) (Fig. 7). The toxic effect of snake venom is further complicated by the inflammatory reaction that is established soon after snakebite accidents is an important process, since besides the toxins in the area of the bite, there is also the involvement of chemical messengers induced by these toxins, such as IL-1, IL-6 and IL-8, which can aid in pathophysiological effects (Ahmed et al., 2008; Gutierrez et al., 2009; Voronov et al., 1999). In mice, ColTx-I induced a systemic interleukin-6 response upon intramuscular injection (Fig. 8). Some studies have reported that myotoxic PLA_2s can act as pro-inflammatory mediators, promoting the secretion of cytokines, which participate in the inflammatory response and, thus, mediate the evolution of local pathological alterations and regeneration (Oliveira et al., 2009; Teixeira et al., 2003).

In conclusion, this D49-PLA_2 myotoxin from *C. oreganus lutosus,* isolated through two chromatographic steps, induced both local and systemic myotoxicity, edema and pro-inflammatory cytokine

IL-6 release, suggesting its active role in the pathogenesis of local tissue damage. Functional versatility and biochemical characterization of ColTx-I provided insights that can be used for the understanding of the mechanism of venom action and elucidation of structural determinants. These insights are important for the development of new approaches to inhibit crotalic snake venom myotoxins, for the improvement of serum therapy and for the use of ColTx-I as a biotechnological tool for studies of muscle injury and repair.

Conflicts of interest

The authors declare no conflict of interest.

Acknowledgments

The authors express their gratitude to CAPES (Coordenação de Aperfeiçoamento de Pessoal de Nível Superior) and CNPq (Conselho Nacional de Desenvolvimento Científico e Tecnológico), FAPESP (Fundação de Amparo a Pesquisa do Estado de São Paulo) for financial support.

Transparency document

Transparency document related to this article can be found online at http://dx.doi.org/10.1016/j.toxicon.2016.03.008.

References

Ahmed, S.M., Ahmed, M., Nadeem, A., Mahajan, J., Choudhary, A., Pal, J., 2008. Emergency treatment of a snake bite: pearls from literature. J. Emerg. Trauma Shock 1, 97–105.

Aird, S.D., Watanabe, Y., Villar-Briones, A., Roy, M.C., Terada, K., Mikheyev, A.S., 2013. Quantitative high-throughput profiling of snake venom gland transcriptomes and proteomes (*Ovophis okinavensis* and *Protobothrops flavoviridis*). BMC Genom. 14, 790.

Ashton, K.G., De Queiroz, A., 2001. Molecular systematics of the western rattlesnake, *Crotalus viridis* (Viperidae), with comments on the utility of the D-loop in phylogenetic studies of snakes. Mol. Phylogenet Evol. 21, 176–189.

Bouchier, C., Ducancel, F., Guignery-Frelat, G., Bon, C., Boulain, J.C., Menez, A., 1988. Cloning and sequencing of cDNAs encoding the two subunits of Crotoxin. Nucleic Acids Res. 16, 9050.

Calderon, L.A., Sobrinho, J.C., Zaqueo, K.D., de Moura, A.A., Grabner, A.N., Mazzi, M.V., Marcussi, S., Nomizo, A., Fernandes, C.F.C., Zuliani, J.P., Carvalho, B.M.A., Da Silva, S.L., Stábeli, R.G., Soares, A.M., 2014. Antitumoral activity of snake venom proteins: new trends in cancer therapy. BioMed Res. Int. 2014, 19.

Calgarotto, A.K., Damico, D.C., Ponce-Soto, L.A., Baldasso, P.A., Da Silva, S.L., Souza, G.H., Eberlin, M.N., Marangoni, S., 2008. Biological and biochemical characterization of new basic phospholipase A_2 BmTX-I isolated from *Bothrops moojeni* snake venom. Toxicon 51, 1509–1519.

Calvete, J.J., 2009. Venomics: digging into the evolution of venomous systems and learning to twist nature to fight pathology. J. Proteom. 72, 121–126.

Carvalho, B.M.A., Santos, J.D.L., Xavier, B.M., Almeida, J.R., Resende, L.M., Martins, W., Marcussi, S., Marangoni, S., Stábeli, R.G., Calderon, L.A., Soares, A.M., Da Silva, S.L., Marchi-Salvador, D.P., 2013. Snake venom PLA_2s inhibitors isolated from brazilian plants: synthetic and natural molecules. BioMed Res. Int. 2013, 8.

Castillo, J., Vargas, L., Segura, C., Gutiérrez, J., Pérez, J., 2012. In vitro antiplasmodial activity of phospholipases A_2 and a phospholipase homologue isolated from the venom of the snake *Bothrops asper*. Toxins 4, 1500.

Cecilio, A., Caldas, S., Oliveira, R., Santos, A., Richardson, M., Naumann, G., Schneider, F., Alvarenga, V., Estevão-Costa, M., Fuly, A., Eble, J., Sanchez, E., 2013. Molecular characterization of Lys49 and Asp49 phospholipases A_2 from snake venom and their antiviral activities against dengue virus. Toxins 5, 1780.

Chacur, M., Longo, I., Picolo, G., Gutierrez, J.M., Lomonte, B., Guerra, J.L., Teixeira, C.F., Cury, Y., 2003. Hyperalgesia induced by Asp49 and Lys49 phospholipases A_2 from *Bothrops asper* snake venom: pharmacological mediation and molecular determinants. Toxicon 41, 667–678.

Chang, L.S., Lin, S.R., Chang, C.C., 1997. Probing calcium ion-induced conformational changes of Taiwan cobra phospholipase A_2 by trinitrophenylation of lysine residues. J. Protein Chem. 16, 51–57.

Chen, Y.H., Wang, Y.M., Hseu, M.J., Tsai, I.H., 2004. Molecular evolution and structure-function relationships of crotoxin-like and asparagine-6-containing phospholipases A_2 in pit viper venoms. Biochem. J. 381, 25–34.

Cho, W., Kezdy, F.J., 1991. Chromogenic substrates and assay of phospholipases A_2. Methods Enzymol. 197, 75–79.

Da Silva, S.L., Almeida, J.R., Resende, L.M., Martins, W., Henriques, F.A.F.A., Baldasso, P.A., Soares, A.M., Taranto, A.G., Resende, R.R., Marangoni, S., Dias-Junior, C.A., 2011. Isolation and characterization of a natriuretic peptide from *Crotalus oreganus abyssus* (Grand Canyon rattlesnake) and its effects on systemic blood pressure and nitrite levels. Int. J. Pept. Res. Ther. 17, 165–173.

Da Silva, S.L., Calgarotto, A.K., Maso, V., Damico, D.C., Baldasso, P., Veber, C.L., Villar, J.A., Oliveira, A.R., Comar Jr., M., Oliveira, K.M., Marangoni, S., 2009. Molecular modeling and inhibition of phospholipase A_2 by polyhydroxy phenolic compounds. Eur. J. Med. Chem. 44, 312–321.

Da Silva, S.L., Comar, M., Oliveira, K.M.T., Chaar, J.S., Bezerra, E.R.M., Calgarotto, A.K., Baldasso, P.A., Veber, C.L., Villar, J.A.F.P., Oliveira, A.R.M., Marangoni, S., 2008. Molecular modeling of the inhibition of enzyme PLA_2 from snake venom by dipyrone and 1-phenyl-3-methyl-5-pyrazolone. Int. J. Quantum Chem. 108, 2576–2585.

Damico, D.C., Da Cruz Hofling, M.A., Cintra, M., Leonardo, M.B., Calgarotto, A.K., Da Silva, S.L., Marangoni, S., 2008. Pharmacological study of edema and myonecrosis in mice induced by venom of the bushmaster snake *Lachesis muta muta* and its basic Asp49 phospholipase A_2 (LmTX-I). Protein J. 27, 384–391.

Damico, D.C., Lilla, S., De Nucci, G., Ponce-Soto, L.A., Winck, F.V., Novello, J.C., Marangoni, S., 2005. Biochemical and enzymatic characterization of two basic Asp49 phospholipase A_2 isoforms from *Lachesis muta muta* (Surucucu) venom. Biochim. Biophys. Acta 1726, 75–86.

Damico, D.C.S., Vassequi-Silva, T., Torres-Huaco, F.D., Nery-Diez, A.C.C., De Souza, R.C.G., Da Silva, S.L., Vicente, C.P., Mendes, C.B., Antunes, E., Werneck, C.C., Marangoni, S., 2012. LmrTX, a basic PLA_2 (D49) purified from *Lachesis muta rhombeata* snake venom with enzymatic-related antithrombotic and anticoagulant activity. Toxicon 60, 773–781.

Diz Filho, E.B., Marangoni, S., Toyama, D.O., Fagundes, F.H., Oliveira, S.C., Fonseca, F.V., Calgarotto, A.K., Joazeiro, P.P., Toyama, M.H., 2009. Enzymatic and structural characterization of new PLA_2 isoform isolated from white venom of *Crotalus durissus ruruima*. Toxicon 53, 104–114.

Edman, P., 1950. Method for determination of the amino acid sequence in peptides. Acta Chem. Scand. 4, 283–293.

Faure, G., Xu, H., Saul, F.A., 2011. Crystal structure of crotoxin reveals key residues involved in the stability and toxicity of this potent heterodimeric beta-neurotoxin. J. Mol. Biol. 412, 176–191.

Fernandez, J., Gutiérrez, J.M., Angulo, Y., Sanz, L., Juárez, P., Calvete, J.J., Lomonte, B., 2010. Isolation of an acidic phospholipase A_2 from the venom of the snake *Bothrops asper* of Costa Rica: biochemical and toxicological characterization. Biochimie 92, 273–283.

Forst, S., Weiss, J., Blackburn, P., Frangione, B., Goni, F., Elsbach, P., 1986. Amino acid sequence of a basic *Agkistrodon halys blomhoffii* phospholipase A_2. Possible role of NH2-terminal lysines in action on phospholipids of *Escherichia coli*. Biochemistry 25, 4309–4314.

Gibbs, H.L., Rossiter, W., 2008. Rapid evolution by positive selection and gene gain and loss: PLA_2 venom genes in closely related *Sistrurus* rattlesnakes with divergent diets. J. Mol. Evol. 66, 151–166.

Gutierrez, J.M., Lomonte, B., 2013. Phospholipases A_2: unveiling the secrets of a functionally versatile group of snake venom toxins. Toxicon 62, 27–39.

Gutierrez, J.M., Ownby, C.L., 2003. Skeletal muscle degeneration induced by venom phospholipases A_2: insights into the mechanisms of local and systemic myotoxicity. Toxicon 42, 915–931.

Gutierrez, J.M., Rucavado, A., Chaves, F., Diaz, C., Escalante, T., 2009. Experimental pathology of local tissue damage induced by *Bothrops asper* snake venom. Toxicon 54, 958–975.

Hernandez, R., Cabalceta, C., Saravia-Otten, P., Chaves, A., Gutierrez, J.M., Rucavado, A., 2011. Poor regenerative outcome after skeletal muscle necrosis induced by *Bothrops asper* venom: alterations in microvasculature and nerves. PLoS One 6, e19834.

Higuchi, D.A., Barbosa, C.M., Bincoletto, C., Chagas, J.R., Magalhaes, A., Richardson, M., Sanchez, E.F., Pesquero, J.B., Araujo, R.C., Pesquero, J.L., 2007a. Purification and partial characterization of two phospholipases A_2 from *Bothrops leucurus* (white-tailed-jararaca) snake venom. Biochimie 89, 319–328.

Higuchi, D.A., Barbosa, C.M.V., Bincoletto, C., Chagas, J.R., Magalhaes, A., Richardson, M., Sanchez, E.F., Pesquero, J.B., Araujo, R.C., Pesquero, J.L., 2007b. Purification and partial characterization of two phospholipases A_2 from *Bothrops leucurus* (white-tailed-jararaca) snake venom. Biochimie 89, 319–328.

Holzer, M., Mackessy, S.P., 1996. An aqueous endpoint assay of snake venom phospholipase A_2. Toxicon 34, 1149–1155.

Kaiser, I.I., Gutierrez, J.M., Plummer, D., Aird, S.D., Odell, G.V., 1990. The amino acid sequence of a myotoxic phospholipase from the venom of *Bothrops asper*. Arch. Biochem. Biophys. 278, 319–325.

Kini, R.M., 2003. Excitement ahead: structure, function and mechanism of snake venom phospholipase A_2 enzymes. Toxicon 42, 827–840.

Kini, R.M., Evans, H.J., 1989. A model to explain the pharmacological effects of snake venom phospholipases A_2. Toxicon 27, 613–635.

Laemmli, U.K., 1970. Cleavage of structural proteins during the assembly of the head of bacteriophage T4. Nature 227, 680–685.

Mackessy, S.P., 2010. Evolutionary trends in venom composition in the Western Rattlesnakes (*Crotalus viridis* sensu lato): toxicity vs. tenderizers. Toxicon 55, 1463–1474.

Mamede, C.C., De Queiroz, M.R., Fonseca, K.C., De Morais, N.C., Filho, S.A., Beletti, M.E., Stanziola, L., De Oliveira, F., 2013. Histological and ultrastructural analyses of muscle damage induced by a myotoxin isolated from *Bothrops alternatus* snake venom. Protein Pept. Lett. 20, 192–199.

Martins, W., Baldasso, P.A., Honório, K.M., Maltarollo, V.G., Ribeiro, R.I.M.A., Carvalho, B.M.A., Calderon, L.A., Stábeli, R.G., Caballol, M.A.O., Acosta, G.A., Oliveira, E., Soares, A.M., Marangoni, S., Albericio, F., Da Silva, S.L., 2014. A novel phospholipase A_2 (D49) from the venom of the *Crotalus oreganus abyssus* (North American Grand Canyon rattlesnake). BioMed Res. Int. 2014, 8.

Mezna, M., Ahmad, T., Chettibi, S., Drainas, D., Lawrence, A.J., 1994. Zinc and barium inhibit the phospholipase A_2 from *Naja naja atra* by different mechanisms. Biochem. J. 301, 503–508.

Montecucco, C., Gutierrez, J.M., Lomonte, B., 2008. Cellular pathology induced by snake venom phospholipase A_2 myotoxins and neurotoxins: common aspects of their mechanisms of action. Cell Mol. Life Sci. 65, 2897–2912.

Murakami, M., Lambeau, G., 2013. Emerging roles of secreted phospholipase A_2 enzymes: an update. Biochimie 95, 43–50.

Murakami, M.T., Arni, R.K., 2003. A structure based model for liposome disruption and the role of catalytic activity in myotoxic phospholipase A_2s. Toxicon 42, 903–913.

Murakami, M.T., Arruda, E.Z., Melo, P.A., Martinez, A.B., Calil-Elias, S., Tomaz, M.A., Lomonte, B., Gutierrez, J.M., Arni, R.K., 2005. Inhibition of myotoxic activity of *Bothrops asper* myotoxin II by the anti-trypanosomal drug suramin. J. Mol. Biol. 350, 416–426.

Nunes, D.C., Rodrigues, R.S., Lucena, M.N., Cologna, C.T., Oliveira, A.C., Hamaguchi, A., Homsi-Brandeburgo, M.I., Arantes, E.C., Teixeira, D.N., Ueira-Vieira, C., Rodrigues, V.M., 2011. Isolation and functional characterization of proinflammatory acidic phospholipase A_2 from *Bothrops leucurus* snake venom. Comp. Biochem. Physiol. C Toxicol. Pharmacol. 154, 226–233.

Oliveira, C.F., Lopes, D.S., Mendes, M.M., Homsi-Brandeburgo, M.I., Hamaguchi, A., De Alcantara, T.M., Clissa, P.B., Rodrigues, V.M., 2009. Insights of local tissue damage and regeneration induced by BnSP-7, a myotoxin isolated from *Bothrops (neuwiedi) pauloensis* snake venom. Toxicon 53, 560–569.

Ponraj, D., Gopalakrishnakone, P., 1996. Establishment of an animal model for myoglobinuria by use of a myotoxin from *Pseudechis australis* (king brown snake) venom in mice. Lab. Anim. Sci. 46, 393–398.

Romero, L., Marcussi, S., Marchi-Salvador, D.P., Silva Jr., F.P., Fuly, A.L., Stabeli, R.G., Da Silva, S.L., Gonzalez, J., Monte, A.D., Soares, A.M., 2010. Enzymatic and structural characterization of a basic phospholipase A_2 from the sea anemone *Condylactis gigantea*. Biochimie 92, 1063–1071.

Saitou, N., Nei, M., 1987. The neighbor-joining method: a new method for reconstructing phylogenetic trees. Mol. Biol. Evol. 4, 406–425.

Salvador, G.H., Fernandes, C.A., Correa, L.C., Santos-Filho, N.A., Soares, A.M., Fontes, M.R., 2009. Crystallization and preliminary X-ray diffraction analysis of crotoxin B from *Crotalus durissus collilineatus* venom. Acta Crystallogr. Sect. F. Struct. Biol. Cryst. Commun. 65, 1011–1013.

Samel, M., Vija, H., Kurvet, I., Künnis-Beres, K., Trummal, K., Subbi, J., Kahru, A., Siigur, J., 2013. Interactions of PLA_2s from *Vipera lebetina*, Vipera berus *berus* and *Naja naja oxiana* venom with platelets, bacterial and Cancer cells. Toxins 5, 203.

Schaloske, R.H., Dennis, E.A., 2006. The phospholipase A_2 superfamily and its group numbering system. Biochim. Biophys. Acta 1761, 1246–1259.

Silveira, L.B., Marchi-Salvador, D.P., Santos-Filho, N.A., Silva Jr., F.P., Marcussi, S., Fuly, A.L., Nomizo, A., Da Silva, S.L., Stabeli, R.G., Arantes, E.C., Soares, A.M., 2013. Isolation and expression of a hypotensive and anti-platelet acidic phospholipase A_2 from *Bothrops moojeni* snake venom. J. Pharm. Biomed. Anal. 73, 35–43.

Sunagar, K., Undheim, E.A., Scheib, H., Gren, E.C., Cochran, C., Person, C.E., Koludarov, I., Kelln, W., Hayes, W.K., King, G.F., Antunes, A., Fry, B.G., 2014. Intraspecific venom variation in the medically significant Southern Pacific Rattlesnake (*Crotalus oreganus helleri*): biodiscovery, clinical and evolutionary implications. J. Proteom. 99, 68–83.

Tecchio, C., Cassatella, M.A., 2014. Neutrophil-derived cytokines: fact beyond expression. Front. Immunol. 5.

Teixeira, C., Cury, Y., Moreira, V., Picolo, G., Chaves, F., 2009. Inflammation induced by *Bothrops asper* venom. Toxicon 54, 67–76.

Teixeira, C.F., Zamuner, S.R., Zuliani, J.P., Fernandes, C.M., Cruz-Hofling, M.A., Fernandes, I., Chaves, F., Gutierrez, J.M., 2003. Neutrophils do not contribute to local tissue damage, but play a key role in skeletal muscle regeneration, in mice injected with *Bothrops asper* snake venom. Muscle Nerve 28, 449–459.

Terra, A.L.C., Moreira-Dill, L.S., Simões-Silva, R., Monteiro, J.R.N., Cavalcante, W.L.G., Gallacci, M., Barros, N.B., Nicolete, R., Teles, C.B.G., Medeiros, P.S.M., Zanchi, F.B., Zuliani, J.P., Calderon, L.A., Stábeli, R.G., Soares, A.M., 2015. Biological characterization of the Amazon coral *Micrurus spixii* snake venom: isolation of a new neurotoxic phospholipase A_2. Toxicon 103, 1–11.

Tonello, F., Simonato, M., Aita, A., Pizzo, P., Fernandez, J., Lomonte, B., Gutierrez, J.M., Montecucco, C., 2012. A Lys49-PLA_2 myotoxin of *Bothrops asper* triggers a rapid death of macrophages that involves autocrine purinergic receptor signaling. Cell Death Dis. 3, e343.

Toyama, M.H., de Oliveira, D.G., Beriam, L.O., Novello, J.C., Rodrigues-Simioni, L., Marangoni, S., 2003. Structural, enzymatic and biological properties of new PLA_2 isoform from *Crotalus durissus terrificus venom*. Toxicon 41, 1033–1038.

Van, D., De Haas, G.H., 1963. The substrate specificity of phospholipase A. Biochim. Biophys. Acta 70, 538–553.

Vargas, L.J., Londoño, M., Quintana, J.C., Rua, C., Segura, C., Lomonte, B., Núñez, V., 2012. An acidic phospholipase A_2 with antibacterial activity from *Porthidium nasutum* snake venom. Comp. Biochem. Physiol. B Biochem. Mol. Biol. 161, 341–347.

Vieira, L.F., Magro, A.J., Fernandes, C.A., de Souza, B.M., Cavalcante, W.L., Palma, M.S., Rosa, J.C., Fuly, A.L., Fontes, M.R., Gallacci, M., Butzke, D.S., Calderon, L.A., Stabeli, R.G., Giglio, J.R., Soares, A.M., 2013. Biochemical, functional, structural and phylogenetic studies on Intercro, a new isoform phospholipase A_2 from *Crotalus durissus terrificus* snake venom. Biochimie 95, 2365–2375.

Voronov, E., Apte, R.N., Sofer, S., 1999. The systemic inflammatory response syndrome related to the release of cytokines following severe envenomation. J. Venom. Anim. Toxins 5, 5–33.

Yang, Z.M., Guo, Q., Ma, Z.R., Chen, Y., Wang, Z.Z., Wang, X.M., Wang, Y.M., Tsai, I.H., 2015. Structures and functions of crotoxin-like heterodimers and acidic phospholipases A_2 from *Gloydius intermedius* venom: insights into the origin of neurotoxic-type rattlesnakes. J. Proteom. 112, 210–223.

Yu, B.Z., Rogers, J., Nicol, G.R., Theopold, K.H., Seshadri, K., Vishweshwara, S., Jain, M.K., 1998. Catalytic significance of the specificity of divalent cations as KS^* and $kcat^*$ cofactors for secreted phospholipase A_2. Biochemistry 37, 12576–12587.

Zhou, X., Tan, T.-C., Valiyaveettil, S., Go, M.L., Kini, R.M., Velazquez-Campoy, A., Sivaraman, J., 2008. Structural characterization of myotoxic ecarpholin S from *Echis carinatus* venom. Biophys. J. 95, 3366–3380.

Zimmermann, M., Aguilera, F.B., Castellucci, M., Rossato, M., Costa, S., Lunardi, C., Ostuni, R., Girolomoni, G., Natoli, G., Bazzoni, F., Tamassia, N., Cassatella, M.A., 2015. Chromatin remodelling and autocrine TNFα are required for optimal interleukin-6 expression in activated human neutrophils. Nat. Commun. 6.

Zuliani, J.P., Gutierrez, J.M., Casais e Silva, L.L., Coccuzzo Sampaio, S., Lomonte, B., Pereira, C.T.F., 2005. Activation of cellular functions in macrophages by venom secretory Asp-49 and Lys-49 phospholipases A_2. Toxicon 46, 523–532.